Check for updates

Solar RRL

WILEY VCH

Solar RRL

RESEARCH ARTICLE OPEN ACCESS

Combination of Indoor and Outdoor Measurements for the Identification of Degradation Trends in PV Modules

Mariella Rivera[1] | Paul Gebhardt[2] | Anna Heimsath[1]

[1]Analysis, Modules and PV Power Plants, Fraunhofer ISE, Freiburg, Germany | [2]PV Module Degradation Analysis and Modeling, Fraunhofer ISE, Freiburg, Germany

Correspondence: Mariella Rivera (mariella.josefina.rivera.aguilar@ise.fraunhofer.de)

Received: 15 May 2025 | **Revised:** 3 July 2025 | **Accepted:** 4 July 2025

Funding: German Federal Ministry for Economic Affairs and Climate Action, Grant/Award Number: FKz.: 03EE1149A; Nagelschneider Foundation

Keywords: accelerated aging | degradation mechanisms | outdoor measurements | topcon

ABSTRACT

Tunnel oxide passivated contact (TOPCon) photovoltaic (PV) modules are gaining significance in the photovoltaic industry due to their high efficiency. However, concerns about their reliability – particularly regarding moisture ingress and ultraviolet (UV) radiation resistance – persist. This study presents a methodology that combines existing indoor and outdoor measurement approaches to investigate specific degradation mechanisms in TOPCon PV modules, along with a comparative analysis against HJT and PERC technologies. The modules underwent accelerated aging testing involving either damp-heat or UV exposure, followed by outdoor exposure alongside non-aged samples. This approach provided insights into the severity of moisture ingress and its effects on the increase in series resistance and the reduction of fill factor. Additionally, we identified the reduction of V_{OC} as the primary mechanism driving performance decline during UV aging and validated the stabilization behavior in the laboratory, which is equivalent to day/night cycle conditions. Overall, this study enhances our understanding of the degradation processes affecting PV modules and their implications for long-term reliability.

1 | Introduction

Reliability testing and quality assurance have become essential for the growing photovoltaic (PV) industry, particularly to ensure long-term operation with an expected lifespan exceeding 20 years for PV power plants. The International Electrotechnical Commission (IEC) provides standard guidelines for reliability tests, including indoor accelerated aging tests. However, a significant challenge is relating these results to outdoor operations, where climate and operational conditions can significantly affect PV module performance and aging patterns, even within the same technology. Moreover, new questions have arisen regarding the applicability of these tests to emerging PV technologies and their applications (e.g., floating PV, building-, or vehicle-integrated systems). For instance, the same crystalline silicon module technology can experience different operating temperatures depending on its installation: open rack installation typically allows for cooling effects, while roof-integrated systems can lead to high temperatures, sometimes exceeding 100°C, due to insulation effects [1]. These elevated temperatures, driven by the installation conditions, can accelerate degradation processes compared to milder conditions and may even trigger degradation mechanisms not activated by standard tests conducted at lower temperatures, such as 85°C [2].

This is particularly relevant for tunnel oxide passivated contact (TOPCon) PV module technology, which is rapidly gaining market share due to its high efficiencies. However, laboratories report concerns about detected degradation that have not yet been validated in outdoor conditions. For TOPCon, a significant factor contributing to its moisture sensitivity is the silver–aluminum (Ag–Al) paste used for the front-side metallization (for front side fingers and busbars). The aluminum within this paste is highly

This is an open access article under the terms of the Creative Commons Attribution License, which permits use, distribution and reproduction in any medium, provided the original work is properly cited.

© 2025 The Author(s). *Solar RRL* published by Wiley-VCH GmbH.

reactive when exposed to moisture and acidic environments. The reactivity of this aluminum paste makes these conductive elements and points of interconnection susceptible to moisture-induced corrosion, leading to increased resistance and performance degradation [3, 4]. Additionally, the silicon nitride (SiNx) passivation/Si interface on the front side of the cell when absorbing ultraviolet (UV) light leads to the breakage of Si–H bonds. This disruption increases interfacial defect density and carrier recombination, while also triggering hydrogen migration, which can further degrade passivation quality and create additional defects, all contributing to UV-induced degradation [5].

Based on our laboratory results at Fraunhofer ISE, degradation effects due to moisture ingress during damp heat (DH) aging testing have shown a median reduction in power performance of 1.7% after 1000 h of DH. Stronger degradation was observed in polymeric backsheet modules, averaging 5%, while glass–glass modules exhibited lower degradation, averaging 1%. This reduction has been attributed to the corrosion of the cell metallization on the front, accelerated by the formation of acetic acid in the encapsulant. This translates into an increase in contact resistance and a decrease in fill factor (*FF*) [6, 7]. DH testing on TOPCon PV modules reveals a wide range of P_{MPP} degradation, highlighting the critical role of the module manufacturing process and materials. Corrosion is a complex process influenced by many factors, including the nature of the PV module encapsulant (ethylene vinyl acetate – EVA or polyolefin – PO/POE) [6, 7], with the presence of metals such as lead (Pb) in the front metallization glass frits [6], and the design of the PV module, including protective layers (polymer or glass), module size, edge seal, framing, soldering flux, and the formulation of the metallization paste [7, 8]. For TOPCon modules with glass-backsheet designs, losses after 1000 hr of DH can reportedly range from 4% to as high as 65%, depending on the specific encapsulant and backsheet materials, and potential contaminants introduced during handling [8, 9]. TOPCon single-glass PV modules, that incorporate optimized designs, such as backsheets with very low water vapor transmission rate (WVTR) and improved encapsulants, have demonstrated better stability, reporting P_{MPP} losses as low as 0.5% to 2.4% after 1000–2000 h of DH [4]. Generally, glass–glass modules have shown better performance, however, reports indicate losses of 20% after 2000 hr of DH for EVA-encapsulated glass–glass modules [6]. Additionally, modules using laser-assisted firing techniques such as laser-enhanced contact optimization (LECO) to reduce or even exclude Al from the printing pastes have shown a reduction in P_{MPP} of 2.1% (1000 hr DH) [10] In some cases, the use of different encapsulant types, such as thermoplastic polyolefin (TPO) has shown corrosion effects [8]. More recently, studies have explored the use of copper plating instead of aluminum to mitigate corrosion [3]. For HJT PV modules, particularly those with glass-backsheet configurations utilizing EVA encapsulants, extended DH testing have also shown considerable P_{MPP} degradation [11]. Researchers report P_{MPP} losses ranging from 10% to 16% after 1000 h DH, attributed to contaminants introduced during handling [9]. Other studies indicate losses up to 50% after 1500 h to 2500 h of DH, possibly due to the electrochemical reactions involving moisture, cell metallization and soldering flux [12].

Efficiency degradations have been reported following UV dose for TOPCon, with a total UV dose of 120 kWh m^{-2}, an average decrease in performance of 7.87% and up to 9.7% was observed, primarily due to voltage loss, which suggests deterioration of the surface passivation, and can largely variate within the different bills of materials (BOM) and manufacturing process of the PV module [5]. Additionally, our laboratories have analyzed around 20 TOPCon module types and found a decrease in P_{MPP} of 5% for more than 40% of the modules after front UV irradiation of only 60 kWh m^{-2} [13]. It has been suggested that passivation layers based on aluminum oxide and silicon nitride may enhance UV stability. Furthermore, it was found that dark storage after UV aging increases performance losses, although this UV damage can be mitigated after phases of illumination and high temperature [13, 14]. Light soaking improves the efficiency due to the reconstitution of free hydrogen following the breaking of B–H–Si bonds, which enhances passivation [15]. This effect underscores the need for comparisons with field applications to understand the implications of day/night cycles.

Recent open questions regarding the reliability of TOPCon technology have raised concerns, particularly about corrosion and UV-induced degradation (UVID): Do alternative materials (e.g., encapsulant, metallization paste [6, 8], back sheets [4]) provide sufficient long-term protection against moisture and acid-induce corrosion? Are the current handling and manufacturing protocols adequate to prevent contamination that could initiate or accelerate corrosion [8, 16]? In terms of UVID, what are the real-life implications of environmental factors such as operation mode, light, and temperature over time? Are the current standard UV testing protocols adequate for identifying UV degradation [13]? To address these inquiries, we focus on these individual aging mechanisms. During damp heat (DH) (Module Quality Test MQT 13) from IEC 61 215, modules are subjected to 85% relative humidity (RH) and 85°C for 1000 hr to identify degradation effects caused by the high humidity and temperature. Additionally, we utilized a modified procedure from standard IEC 61730-2 for UV aging, incorporating a UV Dose cycle of 60 kWh m^{-2} [17].

While accelerated aging tests are crucial for assessing durability, identifying potential design flaws, and predicting long-term performance degradation, these laboratory protocols typically apply stressors sequentially or in isolation, contrasting with real-world conditions where modules face a complex interplay of multiple stressors simultaneously (e.g., temperature fluctuations, light/dark cycles, mechanical loads, soiling, and corrosive atmospheres) [2]. This difference makes it challenging to directly correlate degradation observed in accelerated tests with specific operational lifetimes or precise degradation rates in the field. Furthermore, predicting the field behavior of PV modules is complicated by the varying magnitude and combination of these stressors, which are highly specific to the diverse climate conditions.

To address these challenges and better understand the transition from controlled laboratory conditions to real-world performance, this study employs a sequential combination approach: individual accelerated laboratory aging followed by outdoor exposure. The initial laboratory aging phase, using distinct stressors such as UV dose or a defined DH cycle, is intended to pre-condition the modules by inducing early-life degradation and a targeted degradation mechanism in a controlled manner. This is valuable for understanding the fundamental aspects of a single failure mode. Once the module is outdoors, the lab-induced degradation is subjected to all environmental stressors simultaneously. This

2367198x, 2025, 16, Downloaded from https://onlinelibrary.wiley.com/doi/10.1002/solr.202500364 by Fraunhofer Ise Inst. Solar Energy Systems, Wiley Online Library on [05/11/2025]. See the Terms and Conditions (https://onlinelibrary.wiley.com/terms-and-conditions) on Wiley Online Library for rules of use; OA articles are governed by the applicable Creative Commons License

transition raises the questions: How does the lab-induced specific degradation mode interact with the complex, multistressor outdoor environment? Will the outdoor conditions accelerate the specific damage, decelerate it, or modify its appearance, thereby offering insights into its progression rate or stabilization? Will new degradation modes be triggered, or will other mechanisms become dominant due to the initial, targeted damage?

This study aims to provide data for validating and refining the stress laboratory protocols. By comparing the evolution of lab-induced damage under real outdoor conditions with known field degradation phenomena, it could validate that these individual lab tests effectively target field-relevant failure modes and accurately reflect their potential severity.

2 | Methodology

2.1 | Sample Selection

We selected three types of bifacial PV modules for the assessment, with some types having more than one manufacturer (denoted by numbering): HJT (H1 and H2), TOPCon (T1, T2, and T3), and PERC (P1). These are commercial PV modules available on the market. Unfortunately, the exact properties of the encapsulants are not known, as these are not indicated on the datasheets. However, we can presume that no UV stabilizer was present in the front encapsulants of PERC and TOPCon modules. As the goal of this study is to show the application of the combined indoor and outdoor methodology on modules of different technologies available on the current market, we aim to cover a wide range of products including full and half-cell technologies. Their characteristics were initially measured in the laboratory at standard test conditions (STC) (Table 1).

We performed two sets of experiments: one for DH aging and the other for UV aging (Figure 1). For each type of PV module, there are four samples. Two samples (M01 and M02), denoted as "new," undergo indoor characterization at STC and non-STC, following the characterization procedures from IEC 61853-1. The other two samples (M03 and M04) undergo an accelerated aging cycle and are characterized at STC before and after. All four samples are then exposed to outdoor conditions where their IV curves are monitored and kept in maximum power point (MPP) for around 8 months starting from summer.

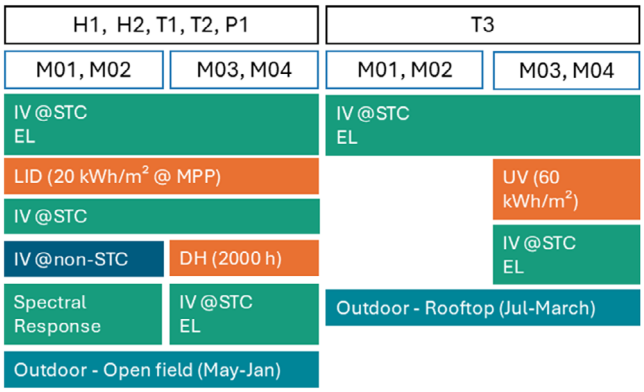

FIGURE 1 | Overview of the methodology. (Left) experiment setup for damp heat aging and (right) ultraviolet aging. This figure includes standard test conditions (STC) (green), non-STC (blue) measurements, and accelerated aging procedures (orange).

2.2 | Indoor Characterization

Indoor characterization was conducted for all samples before and after the accelerated aging, where the IV curve was recorded at STC, along with an electroluminescence (EL) image. For the module types going through the DH experiment setup, the "new samples" received additional characterization at non-STC, following the evaluation guidelines from the standard IEC 61853-1. We measured the IV curves at different levels of irradiance and temperature, also known as power matrix (PM), as well as the angular and spectral responses of the PV modules.

2.3 | Indoor Aging

All samples from the DH setup were first characterized after a light induce degradation (LID) cycle of 20 kWh m^{-2} at MPP, where the laboratory reported a small decrease in P_{MPP} for all types, with a maximum of −0.4% observed in the PERC module. Subsequently, samples M03 and M04 of each module type underwent the DH aging according to standard IEC 61215–2 for two cycles of 1000 h at 85°C and 85% RH, with interim characterization.

The UV aging was conducted using one cycle of 60 kWh m^{-2} exposure with UV-A fluorescent tubes with an intensity of 207 W m^{-2} (315–380 nm) and a fraction of UV-B (280–320 nm) of 5.1% on the front of the PV modules [13]. The modules were then cooled down in the dark, and their IV curve was measured

TABLE 1 | PV Modules parameters measured in laboratory at STC with front illumination and maximum power temperature coefficient (TC PMPP) from datasheet.

	P_{MPP} [W]	V_{OC} [V]	I_{SC} [A]	$TC\ P_{MPP}$ [%°C^{-1}]	Cell type	
H1	391.7	40.0	12.2	−0.26	n-type	Half cell
H2	428.5	40.3	13.0	−0.26	n-type	Half cell
T1	423.2	39.1	13.4	−0.35	n-type	Half cell
T2	412.0	38.9	13.1	−0.30	n-type	Half cell
T3	571.5	52.1	13.5	−0.28	n-type	Half cell
P1	491.2	43.3	14.4	−0.34	p-type	Shingled

2367198x, 2025, 16, Downloaded from https://onlinelibrary.wiley.com/doi/10.1002/solr.202500364 by Fraunhofer Ise Inst. Solar Energy Systems, Wiley Online Library on [05/11/2025]. See the Terms and Conditions (https://onlinelibrary.wiley.com/terms-and-conditions) on Wiley Online Library for rules of use; OA articles are governed by the applicable Creative Commons License

at STC on the following day after a light stabilization procedure at 1000 W for 5 min.

2.4 | Outdoor Exposure

For outdoor characterization, each PV module sample was connected to a programmable electronic load and operated at their MPP. The IV curves were recorded simultaneously every 5 min. The monitoring stations include irradiance measurements on the plane of array (POA) from a thermopile pyranometer and silicon reference cell. A complete weather monitoring station recorded 1-min averages of ambient temperature, wind speed, and relative humidity. Each PV module also had a temperature sensor (PT100) attached to its back.

The module types from the DH experiment setup were exposed to outdoor conditions after indoor characterization and aging. The samples were installed in an open field monitoring station at the Fraunhofer ISE "Outdoor Performance Lab" in Merdingen, Germany. The PV modules are mounted on an open rack system with 30° tilt angle facing south, with the new samples (M01 and M02) on the north row and lab-aged samples (M03 and M04) on the south row (Figure 2). A reference cell on the back of the north row measured the rear-side irradiance. For the module type after the UV aging experiment, the samples were exposed at our rooftop monitoring station in Freiburg, Germany. Due to the inhomogeneity of the conditions, it was not possible to measure the rear irradiance adequately; therefore, we covered the back of the modules with wood material leaving approximately 10 cm of spacing, to compare monofacial module behavior.

2.5 | Data Handling

The IV curve data provides characteristics values of I_{SC}, V_{OC}, P_{MPP}, I_{MPP}, V_{MPP}, *FF*, and series resistance (*Rs*), which is calculated as the IV curve slope at the point of V_{OC}. To compare between PV module types and laboratory measurements, quality checks, filtering, translation, and normalization of the data are necessary. This process helps to reduce the effect of measurement uncertainties, which have been previously analyzed at both types of monitoring stations from Fraunhofer ISE, where P_{MPP} measurement uncertainties reach 3.3% ($k = 2$) in open field conditions and up to 5.7% ($k = 2$) on roof top monitoring. These uncertainties were mainly correlated with irradiance variations at high angle of incidence (AOI) and partial shading effects [18]. In our study, we do not account from sources of partial shading, but nevertheless we look for stable irradiance conditions at low AOI. Therefore:

- IV curve measurements are filtered at irradiance ranging between 775 and 825 W m^{-2}, with irradiance and temperature fluctuations during curve acquisition kept below 1% for steady state conditions.
- Parameters are corrected for temperature and irradiance using established correction methods (Equation (1), (2), and (3)) [19]. Corrections are made to a reference irradiance level of $G_0 = 800$ W m^{-2} and nominal module operating temperature (NMOT) of $T_0 = 42.5$°C, using temperature coefficients provided in datasheet.

$$P_{MPP-0} = \left(\frac{G_0}{G}\right)\left(\frac{P_{MPP}}{1+\gamma(T-T_0)}\right) \quad (1)$$

$$I_{SC-0} = \left(\frac{G_0}{G}\right)\left(\frac{Isc}{1+\alpha(T-T_0)}\right) \quad (2)$$

$$V_{OC-0} = \frac{Voc}{1+\beta(T-T_0)}\left(1+\delta \ln \frac{G_0}{G}\right) \quad (3)$$

where G is the total irradiance (front + rear) (W m^{-2}), T is the measured module temperature (°C), δ is the irradiance coefficient for V_{OC} (%), γ, α, β are the temperature coefficients (%/°C) for P_{MPP}, I_{SC} and V_{OC}, respectively.

- Parameters are normalized to initial laboratory measurements at non-STC ($N\,P_{MPP-0}$, $N\,I_{SC-0}$, $N\,V_{OC-0}$) levels of 800 W m^{-2} and 42.5°C. These non-STC values were measured in the laboratory according to IEC 61 853-1: "Procedure for irradiance and temperature performance measurements" to facilitate comparisons with real outdoor conditions.

The outdoor degradation is denoted as the percentage difference in performance between the parameters of the new and lab-aged

FIGURE 2 | Outdoor exposure for damp heat experiment (left) and for ultraviolet aging experiment (right) at Fraunhofer ISE outdoor performance lab.

2367198x, 2025, 16, Downloaded from https://onlinelibrary.wiley.com/doi/10.1002/solr.202500364 by Fraunhofer Ise Inst. Solar Energy Systems, Wiley Online Library on [05/11/2025]. See the Terms and Conditions (https://onlinelibrary.wiley.com/terms-and-conditions) on Wiley Online Library for rules of use; OA articles are governed by the applicable Creative Commons License

samples ($P_{MPP,\ aged} - P_{MPP,\ new}$), evaluated over different time intervals (e.g. 1st week and 8th month of exposure). The evolution and behavior of the corrected parameters during the outdoor exposure are evaluated on 15 days average intervals.

3 | Results

3.1 | Outdoor Benchmarking: TOPCon, HJT, and PERC

For the different module types that underwent DH aging, we conducted an initial benchmarking evaluation under outdoor conditions by comparing their performance during the first week of outdoor exposure. Figure 3 shows the corrected and normalized to non-STC maximum power ($N\ P_{MPP-0}$), where the whiskers represent an average standard deviation of 0.8% from the mean for all samples. The interquartile range (IQR) shows a greater performance variability for new samples (e.g., H2 and T1 around 1.5% spread) that have only undergone a 20 kWh m^{-2} light stabilization. This is consistent with findings by Theristis et al. on new PV module technologies, regarding inherent manufacturer differences and varied responses to initial stabilization (as early-life variations). In contrast, lab-aged samples show reduced variability in some module types (e.g., IQR around 0.8% for H1 and T2). This might suggest that the cumulative stressors, from the DH cycle, may induce a "settling" or stable performance, as internal materials and interfaces reach a more stable, nevertheless degraded equilibrium. This observed behavior, where different stress histories lead to varied performance distributions, highlights the importance of long-term outdoor exposure for capturing stable PV module behaviors, which Theristis et al. identify as crucial for accurate long-term degradation rate estimations and understanding nonlinear performance evolution [20].

In the case of the T3 modules undergoing UV-aging cycle, the new samples exhibited stable performance ($N\,P_{MPP-0}$). We attributed the above to initial conditions effect seen for the new samples to the influence of rear side irradiance, which may not be completely ruled out due to our backside cover on the rooftop installation for these bifacial PV modules (Figure S16). The data shows an average standard deviation of 0.8% across all samples; therefore, we assume an equal influence, allowing for relative comparisons between them under outdoor conditions. In this context, the lab-aged samples performed approximately 2.4% lower during the first week of exposure (Figure 4).

3.2 | Indoor versus Outdoor Performance Differences

To compare the degradation observed under laboratory conditions (aged-initial performance) with the PV degradation observed in the field, we analyzed the difference in P_{MPP} between new and lab-aged samples under stable outdoor conditions. This was done

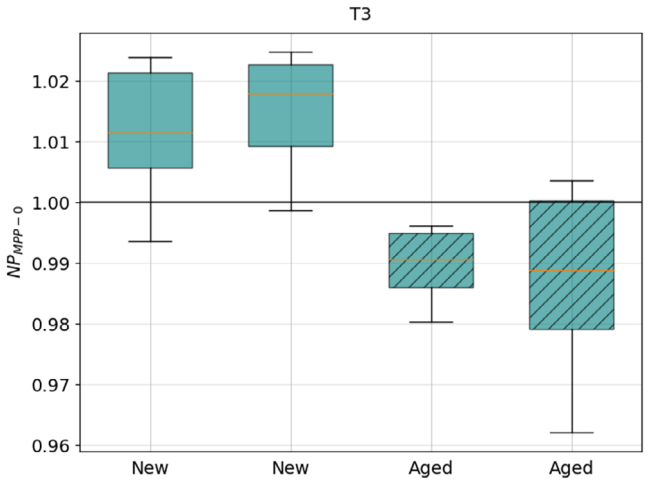

FIGURE 4 | Performance corrected and normalized to initial laboratory conditions at non-STC ($N\,P_{MPP-0}$) on the first week of outdoor exposure for TOPCon -T3 new and lab-aged samples (dashed boxplots) undergoing UV aging.

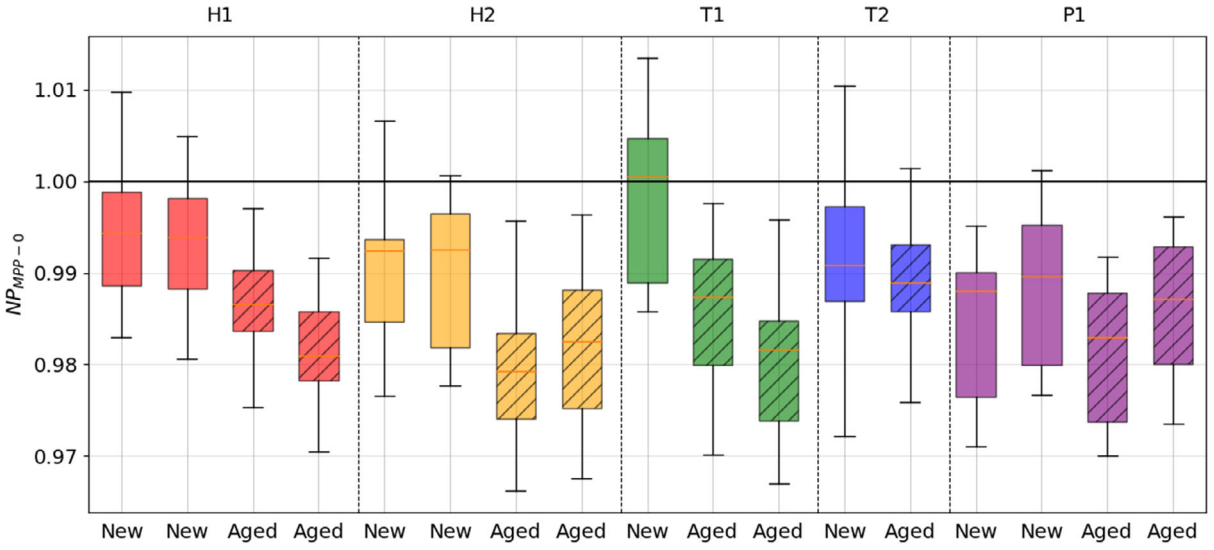

FIGURE 3 | Performance ($N\,P_{MPP-0}$) during the first week of outdoor exposure for the PV modules undergoing DH aging experiment. Lab-aged samples are represented by dashed boxplots. Missing samples for T1 and T2 were removed due to clear technical issues.

23671986, 2025, 16, Downloaded from https://onlinelibrary.wiley.com/doi/10.1002/solr.202500364 by Fraunhofer Ise Inst. Solar Energy Systems, Wiley Online Library on [05/11/2025]. See the Terms and Conditions (https://onlinelibrary.wiley.com/terms-and-conditions) on Wiley Online Library for rules of use; OA articles are governed by the applicable Creative Commons License

either by comparing the relative difference between aged and new samples ($P_{MPP\ aged\text{-}new}$), or by assessing the changes from initial performance with respect to the new samples. In the relative comparison (aged-new), both sets of samples are measured under the same outdoor conditions, therefore, environmental and systematic influences are largely canceled out. However, the 3.3% uncertainty for power measurements in our test field [18] becomes relevant when evaluating the absolute P_{MPP} changes from initial performance. Deviations larger than those observed under controlled laboratory conditions and beyond expected uncertainties may indicate actual degradation of the PV modules.

3.2.1 | Effect of DH Pre-aging

Figure 5 shows the changes in IV characteristic parameters after each step of the indoor experiment (LID, DH 1st and 2nd cycle), with supporting EL images in Figure S7–S11. The PV modules H1, H2, and T1 had the largest decreases in P_{MPP}, ranging from 2.5% to 3%, mainly due to reductions in I_{SC} and *FF*. In contrast, the performance changes for modules T2 and P1 were less (below – 2%), mainly attributed to a decrease in I_{SC}, with no notable change in *FF*.

Furthermore, under the outdoor exposure, Figure 6 shows the performance change for new and lab-aged samples, relative to the initial performance of new samples. After 1 week and 8 months of exposure, the differences between laboratory degradation measurements (after pre-aging in a climate chamber) and outdoor evaluations ($P_{MPP\ aged\text{-}new}$) ranged from 0.5% to 1.7%. However, some *"new samples"* module types showed significant signs of degradation after 8 months of exposure compared to their initial performance, surpassing the reported degradation in the laboratory, such as H2 and P1. Therefore, caution must be taken in the evaluation, as the performance differences between samples may be a results of other degradation mechanisms present in the new samples.

The PERC new samples show a 2% performance reduction compared to the lab-aged samples, primarily due to low values of I_{MPP}

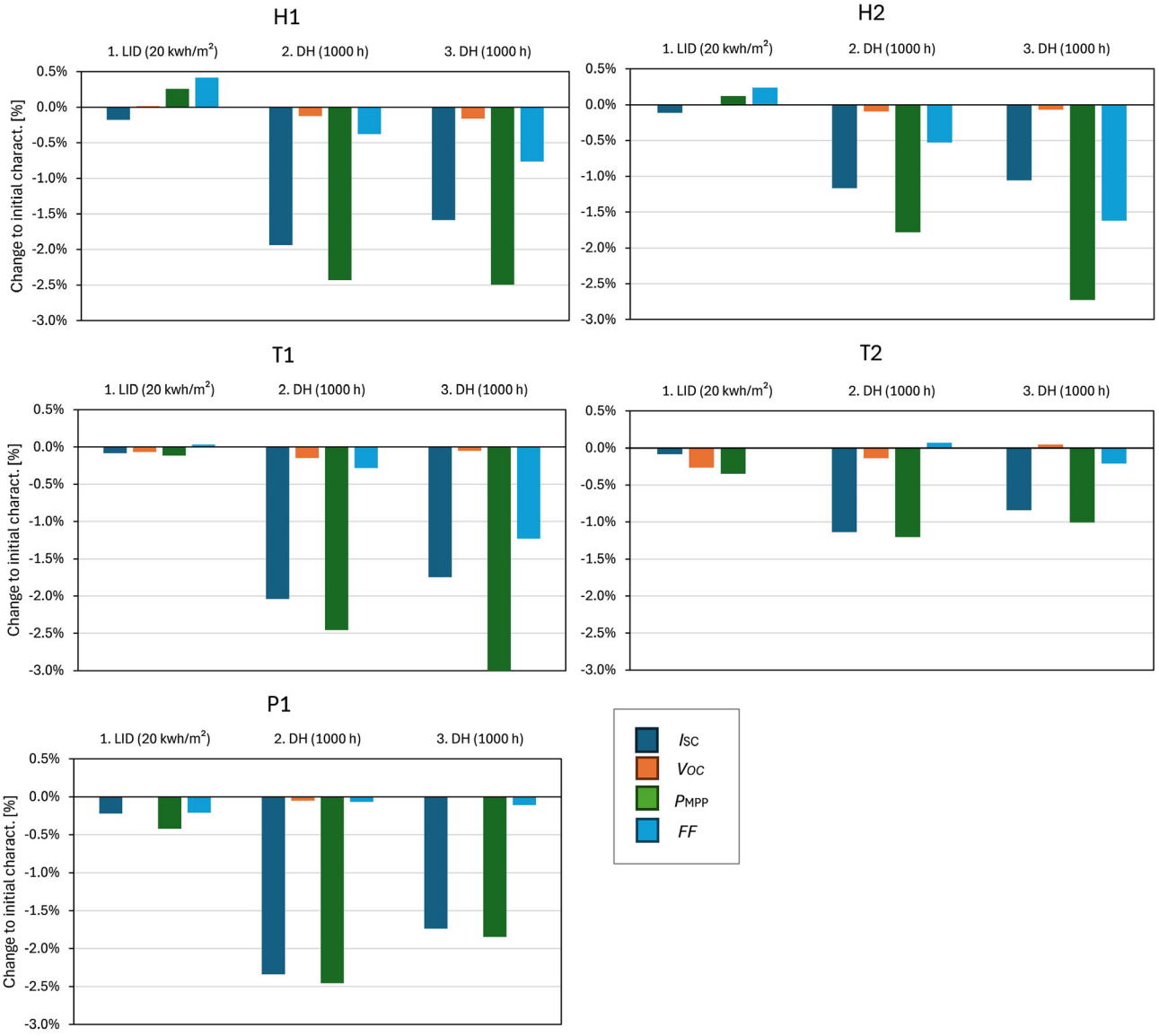

FIGURE 5 | IV characteristic parameters average changes from initial characterization for the lab-aged samples, after each step of the DH aging experiment: 1) LID, 2) DH of 1000 hr, and 3) DH of 1000 hr.

2367198x, 2025, 16, Downloaded from https://onlinelibrary.wiley.com/doi/10.1002/solr.202500364 by Fraunhofer Ise Inst. Solar Energy Systems, Wiley Online Library on [05/11/2025]. See the Terms and Conditions (https://onlinelibrary.wiley.com/terms-and-conditions) on Wiley Online Library for rules of use; OA articles are governed by the applicable Creative Commons License

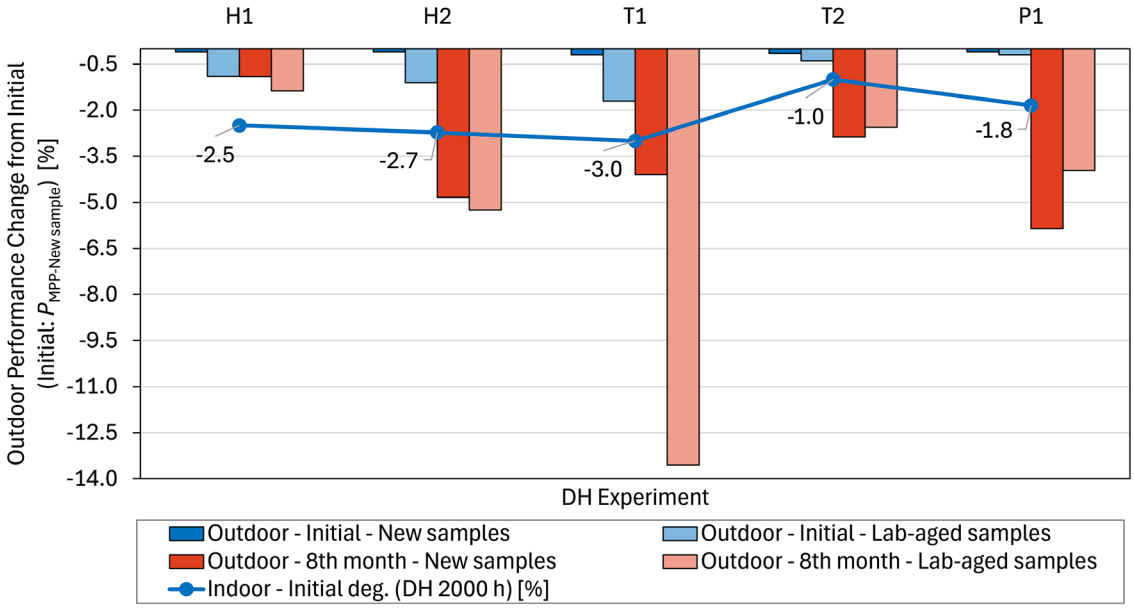

FIGURE 6 | Performance changes due to DH experiment of new samples (M01 and M02) and lab-aged samples (M03 and M04) compared to initial P_{MPP} of new samples. After 1 week and 8 months of outdoor exposure (except for H2 with 4 months), compared to laboratory DH aged samples (M03 and M04) (blue line).

and I_{SC} (Figure S3). Further research is necessary to evaluate this technology under outdoor conditions following DH. While it is known to be a gallium-doped PERC module, some studies suggest that it may still be susceptible to light and elevated temperature-induced degradation (LeTID), though generally to a lesser extent than B-doped cells, with fabrication processes potentially influencing this susceptibility [21].

3.2.2 | Effect of UV Pre-aging

For the TOPCon module type undergoing UV aging (T3), the difference between new and lab-aged samples after 1 week of outdoor exposure aligns with laboratory findings. The laboratory reports after one cycle of 60 kWh m^{-2} and subsequent light stabilization, P_{MPP} reduction of 2.5% and V_{OC} 1.5% (Figure 7) [13].

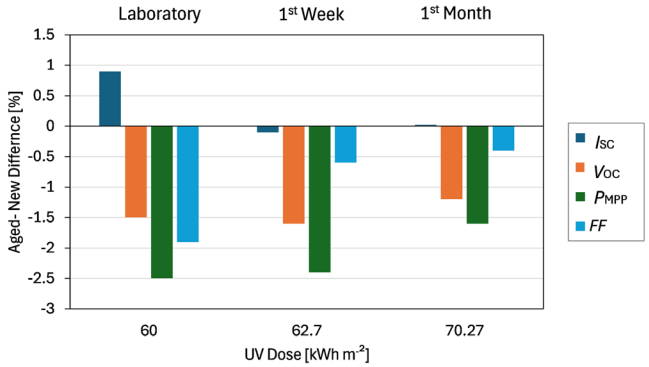

FIGURE 7 | Differences in parameters (I_{SC}, V_{OC}, P_{MPP}, and *FF*) measured in the laboratory before and after UV aging, represented by the left bars at 60 kWh m^{-2}. The right bars illustrate the outdoor performance differences between lab-aged and new samples, with the additional UV dose received outdoors and their stabilization behavior (reduced difference).

During the first week of performance with just an additional 2.7 kWh m^{-2} of UV dose, the relative difference between new and lab-aged samples was −2.4% (P_{MPP}) and −1.6% (V_{OC}). Within the first days of outdoor exposure with natural dark-light cycles, this provided a more realistic scenario for the UV degradation and stabilization effects on this technology, further supporting the laboratory evaluations that now recommend a light stabilization procedure after UV dose. Section 3.3.3 describes all samples behavior after further outdoor exposure.

3.3 | Failure Modes

To identify the driving factor contributing to the degradation of the different PV module types in this study, we analyzed the optical appearance of the modules and the evolution of the main IV characteristics (I_{SC}, V_{OC}, P_{MPP}, *FF*, *Rs*) over the exposure time. All measurements are filtered to a specific irradiance range (see Section 2.5) and compared between new and lab-aged samples.

3.3.1 | Surface Degradation

Some of the PV module types that underwent DH cycles showed cell damage, as indicated by EL images taken after aging cycle (Figure S7–S11). This damage included dark areas mostly at the edges and corners (e.g. T1, T2, H2, and P1), while H1 presented no signs of cell damage. Once the modules were installed outdoors, white and brown vertical dripping marks became visible, which may have originated from the glass. After 5 months of outdoor exposure, the discoloration, dripping marks and brown dots on the front and rear side of all module types lab-aged samples increased (Figure 8, Figure S12-S15).

Both types of HJT modules (H1 and H2) exhibit varying levels of sensibility to moisture, with the main decrease in performance attributed to a reduction in I_{SC} (Figure S1 and S2). Moisture ingress

2367198x, 2025, 16, Downloaded from https://onlinelibrary.wiley.com/doi/10.1002/solr.202500364 by Fraunhofer Ise Inst. Solar Energy Systems, Wiley Online Library on [05/11/2025]. See the Terms and Conditions (https://onlinelibrary.wiley.com/terms-and-conditions) on Wiley Online Library for rules of use; OA articles are governed by the applicable Creative Commons License

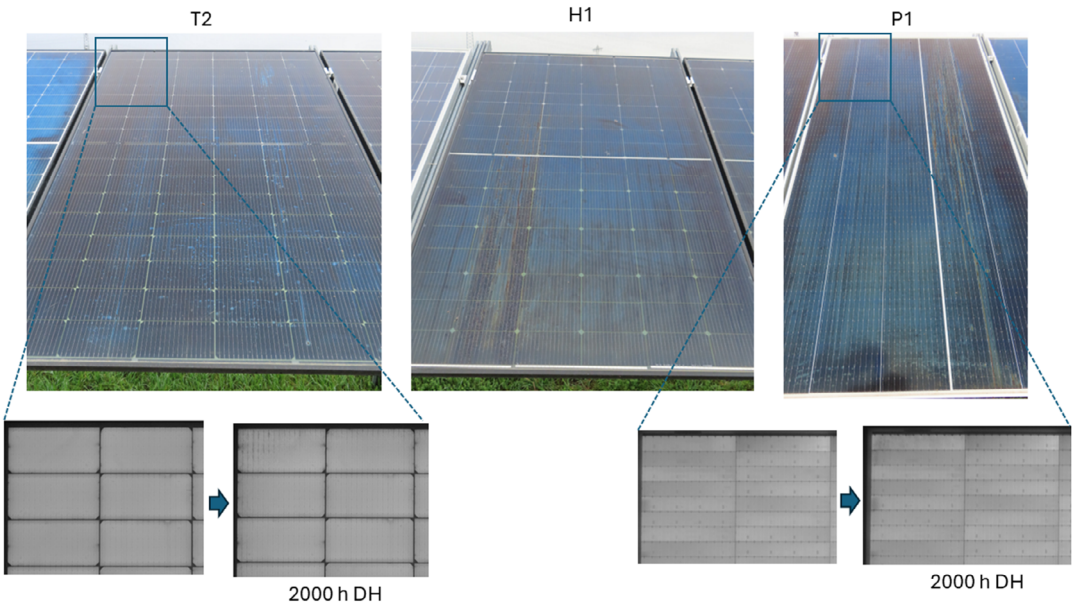

FIGURE 8 | Module types T2, H1, and P1 (left to right), lab-aged samples visual inspection after 5 months of outdoor exposure. Samples underwent 2000 h of DH. Lower images show specific areas before and after DH, with low cell damage at the module corners.

can weaken the adhesive bonds between module layers, potentially leading to issues such as delamination. This was observed in H1 modules, which displayed delamination in the bottom corner cells of both new and lab-aged samples (Figure S15).

The failure effects caused by DH could be a decrease in I_{SC} mainly related to the discoloration of the encapsulant due to the high temperatures and humidity ingress, and further aggravated with more hours of DH (>1000hr) in a FF-reduction with a primary increase in *Rs*, due to corrosion of cells and connectors [22–24].

3.3.2 | Corrosion Degradation

From the DH cycle, it is assumed that all modules have endured some degree of moisture ingress. However, EL images indicate that the two module types that showed significant damage due to this ingress were T1 and H2 (Figure 9). In glass–glass modules, moisture-induced corrosion typically progresses from the edges and corners. This damage is characterized in EL images by darkening of the cell metallization or connectors, which is also reflected in both cases with high values of *Rs*, increasing by up to 20% (Figure S4 and S6). This correlation confirms cell deterioration.

For TOPCon type T2, after 8 months of exposure, there was no significant decrease in P_{MPP} (+0.4%) for the lab-aged samples when compared to the new samples. However, there is a decrease in *FF* of 0.4% (Figure 10), and the lab-aged samples show a higher fluctuation in *Rs*, especially during the hotter months. This fluctuation may be related to how Rs is calculated from the slope to the fit of points close to V_{OC}. The difference in *Rs* between new

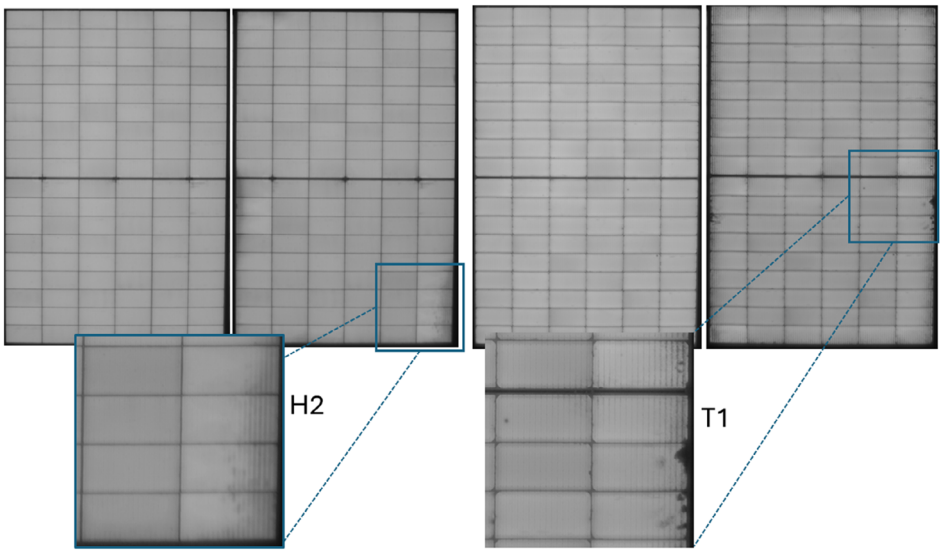

FIGURE 9 | EL images of H2 and T1 modules after 2000h of DH cycle, showing darkening of cells at the edges and corners of the module. The left module is before and the right module after DH cycle.

2367198x, 2025, 16, Downloaded from https://onlinelibrary.wiley.com/doi/10.1002/solr.202500364 by Fraunhofer Ise Inst. Solar Energy Systems, Wiley Online Library on [05/11/2025]. See the Terms and Conditions (https://onlinelibrary.wiley.com/terms-and-conditions) on Wiley Online Library for rules of use; OA articles are governed by the applicable Creative Commons License

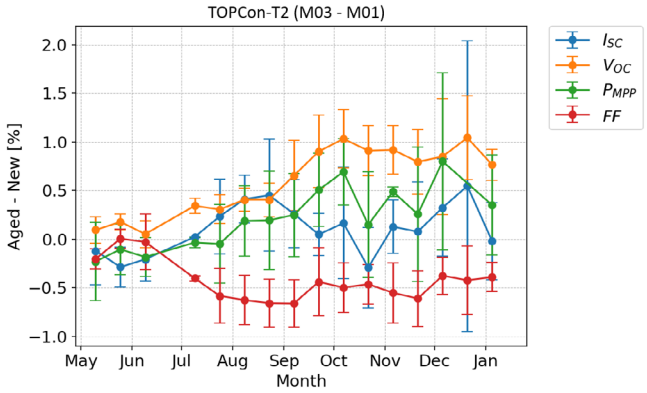

FIGURE 10 | TOPCon-T2 parameters (P_{MPP}, I_{SC}, V_{OC}, and FF) difference between new sample (M01) and lab-aged sample (M03) after the DH cycle, under outdoor exposure, averaged every 15 days.

and lab-aged samples increases over time, reaching up to 7% (Figure S5).

Conversely for TOPCon module type T1, during the 8 months of outdoor exposure P_{MPP} degraded gradually for the lab-aged samples by 9.75%, and FF decreased by 9.4%, related to an increase in Rs around 20% (Figure 11, Figure S6), assuming that the decrease in performance of the new samples is not significant (Figure 6). The results suggest a strong effect of corrosion on the aged samples triggered by the ingress of moisture (as indicated by EL images for T1, Figure S7).

T2 exhibited more stable behavior outdoors, with performance reductions mainly from an increase in Rs (7%) and a subsequent reduction in FF. In contrast, module types H2 and T1 showed signs of damage due to moisture ingress in the EL images, leading to a significant decrease in P_{MPP}, commonly due to a large increase in Rs (20%) during outdoor exposure.

3.3.3 | UV Degradation

The P_{MPP} degradation for the lab-aged samples (M03 and M04) ranged from 2.4% initially to 2% by the 8th month, mainly due to a decrease in V_{OC}, while the new samples (M01 and M02) exhibited a P_{MPP} decrease from initial performance of up to 1%, with a reduction in FF of 0.5%. Figure 12 shows the change in IV characteristic parameters over the 8 months of exposure compared to

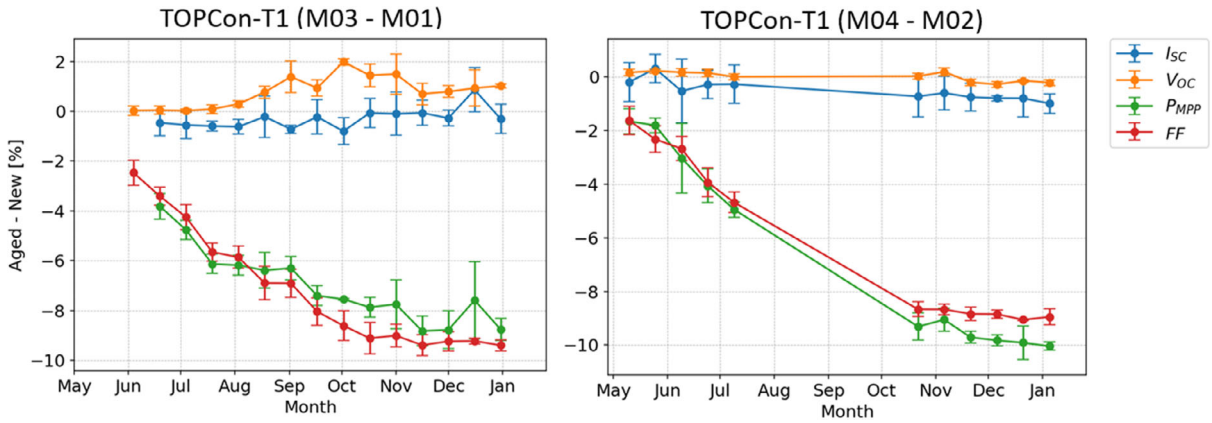

FIGURE 11 | Differences TOPCon- T1 parameters (P_{MPP}, I_{SC}, V_{OC}, FF) between new (M01 and M02) and lab-aged (M03 and M04) samples. Left: M03-M01. Right: M04-M02, under outdoor exposure after DH cycle, averaged every 15 days.

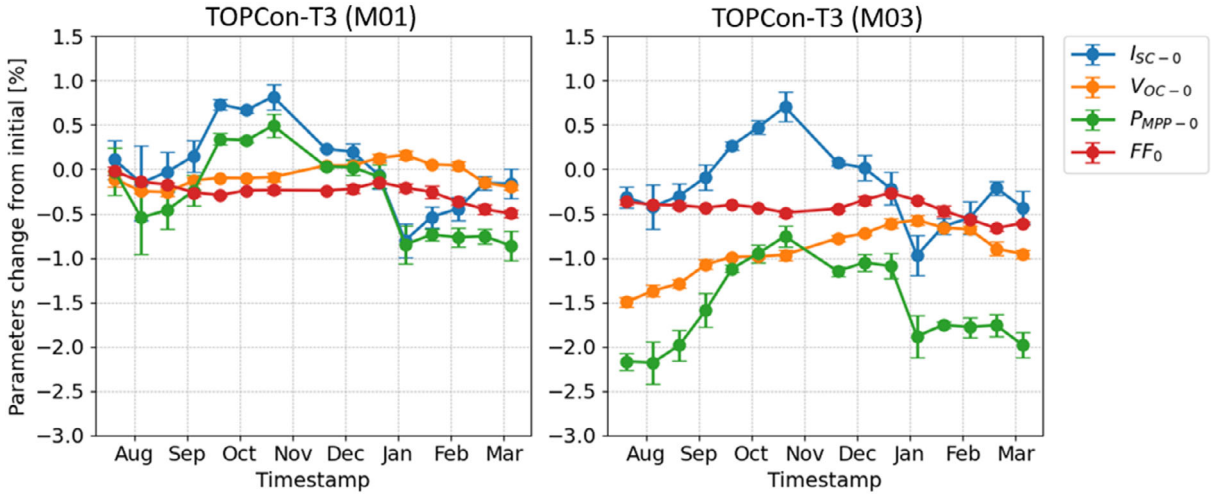

FIGURE 12 | Changes in TOPCon- T3 parameters (P_{MPP-0}, I_{SC-0}, V_{OC-0}, FF_0– temperature and irradiance corrected) compared to the average initial performance of new samples. For new (M01) and lab-aged (M03) samples under outdoor exposure after UV cycle, averaged every 15 days.

23671981, 2025, 16, Downloaded from https://onlinelibrary.wiley.com/doi/10.1002/solr.202500364 by Fraunhofer Ise Inst. Solar Energy Systems, Wiley Online Library on [05/11/2025]. See the Terms and Conditions (https://onlinelibrary.wiley.com/terms-and-conditions) on Wiley Online Library for rules of use; OA articles are governed by the applicable Creative Commons License

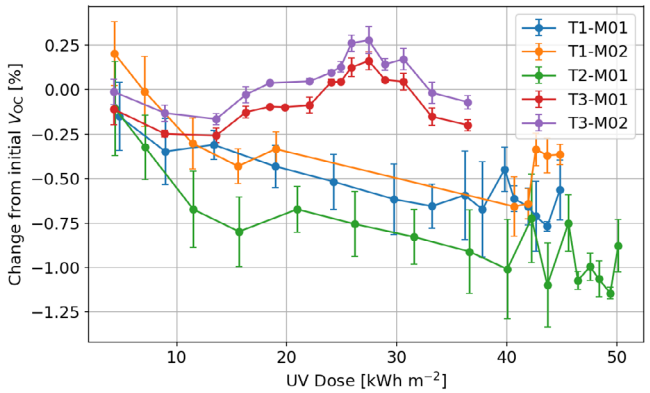

FIGURE 13 | Change in V_{OC} from initial measurement for all TOPCon module types (T1, T2, and T3) of new samples (M01 and M02), throughout the outdoor exposure period and the corresponding UV dose received outdoors.

the initial performance of the new samples. The V_{OC} for the lab-aged samples (M03 and M04) exhibited an increase rate of approximately 0.3% during the first 3 months of exposure, with an average standard deviation (STDev) of 0.04% in the measurements, after which it stabilized. In contrast, the new samples showed a relatively stable and not degraded V_{OC}. This suggests that the lab-aged samples are stabilizing due to V_{OC} changes.

When comparing the V_{OC} decrease of all the TOPCon module types (new samples) (Figure 13), a distinction can be observed between the module type with a covered backside (T3) and those installed on an open rack in the field without a backside cover (T1 and T2). The latter exhibits a larger V_{OC} decrease rate of up to 1%, while the V_{OC} of T3 modules remained stable with a reduction of less than 0.25%. Further research under the same outdoor conditions is necessary to understand the influence of rear-side UV degradation in the field.

4 | Conclusion

The combination of specific accelerated aging cycles followed by outdoor exposure helps to enhance our understanding of the development of targeted degradation mechanisms. By periodically monitoring the IV curves of both new and lab-aged samples, it is possible to identify the changes in parameters causing performance decreases under actual operational conditions. Our findings provide valuable insights into the complex interplay between targeted lab-induced degradation and the multiple stressors of field operation. The results suggest that standard IEC tests, while valuable, may not fully capture the complexity of field degradation. For module developers and end users, this implies that relying solely on IEC testing may lead to either under- or overestimation of potential degradation risks. This was evident in our observations with the TOPCon module T1 (lab-aged), which experienced a significant rapid decrease in performance during outdoor exposure. In contrast, the HJT (H1) modules demonstrated less degradation in the field compared to what was reported in the laboratory conditions after DH. Similarly, our UV experiment revealed that some modules showed signs of stabilization, likely influenced by day/night cycles. This highlights the need for further research under outdoor environments and emphasizes the practical short-term insights that this combined methodology can provide.

Following laboratory DH testing and subsequent outdoor exposure demonstrated that both TOPCon and HJT modules are sensitive to moisture ingress. Both types showed a decrease in I_{SC}, presumably due to damage to the encapsulant layer or changes in the optical properties, influenced by the high temperatures and moisture. The more affected samples showed a reduction in *FF* and an increase in *Rs*, attributed to further cell damage due to moisture ingress and corrosion. These two degradation mechanisms were distinguished and validated following further outdoor exposure.

For TOPCon module type T1, it was confirmed by the manufacturer, as an involved research partner, that polyolefin elastomers (POE) were used as the encapsulant, known in some cases to reduce corrosion degradation. However, our observations indicate that T1 experienced one of the highest amounts of degradation, with a decrease in performance from lab-aged samples of 3% in laboratory and after 8 months of exposure of 9.75%. This suggests that even in the absence of acetic acid for POE, other factors, such as non-optimal lamination processing that releases curing residues or reactive species, polymer additives, or solder flux, could still contribute to moisture sensitivity and corrosion [6, 8]. Furthermore, the initial moisture and heat stress from the DH test likely compromised critical interfaces or materials, creating vulnerabilities that were rapidly exploited. This highlights how initial moisture ingress and related cell damage can act as significant precursor to accelerated field degradation.

UV-induced degradation in TOPCon modules was evident through a decrease in V_{OC}, which later stabilized under outdoor exposure. The transition to the field, with its inherent day/night cycles, appeared to trigger stabilization mechanisms. This behavior aligns with laboratory observations and highlights the need for a stabilization cycle following UV aging in reliability tests. Our initial outdoor measurements validated the performance degradation reported in laboratory after stabilization, with P_{MPP} of 2.5% and V_{OC} of 1.5% for TOPCon-T3. These results may raise further research questions, on whether the high-intensity stress of a lab UV test fully represents the degradation experienced under cyclical real-world UV exposure, where dark periods and temperature variations can influence material responses.

This study emphasizes the need for outdoor monitoring of PV modules to fully understand and quantify degradation processes, which significantly vary based on the module's BOM. Our methodology allowed for the focused initiation of a known degradation mode and the subsequent observation of its specific evolution and interaction with outdoor conditions. As the PV industry has adopted TOPCon technology as mainstream, future research should focus on understanding the impacts of various environmental stressors and exploring alternative BOM and manufacturing processes. A combination of indoor and outdoor evaluations could further determine degradation risks, helping to improve the overall reliability of these advanced technologies and will be further developed. As an outlook of this research is the development of more representative aging protocols by

2367198x, 2025, 16, Downloaded from https://onlinelibrary.wiley.com/doi/10.1002/solr.202500364 by Fraunhofer Ise Inst. Solar Energy Systems, Wiley Online Library on [05/11/2025]. See the Terms and Conditions (https://onlinelibrary.wiley.com/terms-and-conditions) on Wiley Online Library for rules of use; OA articles are governed by the applicable Creative Commons License

incorporating combine-accelerated stress testing in the laboratory phase, which could be validated with our outdoor experiences to improve the accuracy of service life predictions models.

Acknowledgements

Funding was provided by the German Federal Ministry for Economic Affairs and Climate Action (FKz.: 03EE1149A "MiMoRisk"). M.R. is thankful for the financial support of her PhD through Nagelschneider Foundation (Munich, Germany). The authors thank very much the insightful discussions and revisions on content and data analysis provided by Dr. Christian Reise and Erdmut Schnabel, from the Outdoor Performance Lab Team in the PV Power Plants Group at Fraunhofer ISE.

Open Access funding enabled and organized by Projekt DEAL.

Conflicts of Interest

The authors declare no conflicts of interest.

Data Availability Statement

The data that support the findings of this study are available from ["MiMoRisk" Project Partners]. Restrictions apply to the availability of these data, which were used under license for this study. Data are available from the authors with the permission of ["MiMoRisk" Project Partners].

References

1. M. D. Kempe, D. Holsapple, K. Whitfield, and N. Shiradkar, "Standards Development for Modules in High Temperature Micro-Environments," *Progress in Photovoltaics: Research and Applications*, 29 (2021): 445.

2. K.-A. Weiß, E. Klimm, and I. Kaaya, "Accelerated Aging Tests Vs Field Performance of PV Modules," *Prog. Energy*, 4 (2022): 42009.

3. X. Wang, C. Sen, X. Wu, et al., "Alleviating Contaminant-Induced Degradation of TOPCon Solar Cells with Copper Plating," *Solar Energy Materials and Solar Cells* 282 (2025): 113444.

4. Y. Ye, Y. Zhou, Y. Wang, et al., "Damp-Heat Stability Investigation of Glass-Backsheet Modules Based on TOPCon Solar Cells," *Solar Energy Materials and Solar Cells*. (292 (2025): 113764.

5. A. Sinha, J.-N. Jaubert, and T. Karin, Photovoltaic Specialist Conference (PVSC), (IEEE, 2024), 1745–1747.

6. P. M. Sommeling, J. Liu, and J. M. Kroon, "Corrosion Effects in Bifacial Crystalline Silicon PV Modules; Interactions between Metallization and Encapsulation," *Solar Energy Materials and Solar Cells* 256 (2023): 112321.

7. M. Aghaei, A. Fairbrother, A. Gok, et al., "Review of Degradation and Failure Phenomena in Photovoltaic Modules," *Renewable and Sustainable Energy Reviews* 159 (2022): 112160. 1364-0321.

8. C. Sen, H. Wang, M. U. Khan, et al., "Buyer Aware: Three New Failure Modes in TOPCon Modules Absent from PERC Technology," *Solar Energy Materials and Solar Cells*. (272 (2024): 112877.

9. C. Sen, H. Wang, M. U. Khan, et al., "Hidden Traces: Insights into How Solar Cell Handling Drives Damp-Heat Failures in HJT and TOPCon Modules," *Solar Energy Materials and Solar Cells*. (289 (2025): 113695.

10. X. Wu, X. Wang, W. Yang, et al., "Enhancing the Reliability of TOPCon Technology by Laser-Enhanced Contact Firing," *Solar Energy Materials and Solar Cells*. (271 (2024): 112846.

11. A. A. Hasan, A. W. Mahmood Zuhdi, A. M. Al-Ghaili, et al., "A Review on Silicon Photovoltaic Module Degradations and Recent Identification Techniques," *Solar Energy* 288 (2025): 113288.

12. C. Sen, H. Wang, X. Wu, et al., "Four Failure Modes in Silicon Heterojunction Glass-Backsheet Modules," *Solar Energy Materials and Solar Cells*. (257 (2023): 112358.

13. P. Gebhardt, U. Kräling, E. Fokuhl, I. Hädrich, and D. Philipp, "Reliability of Commercial TOPCon PV Modules -- An Extensive Comparative Study," *Prog. Photovolt: Res. Appl* (2024), https://doi.org/10.1002/pip.3868.

14. F. T. Thome, P. Meßmer, S. Mack, et al., "UV-Induced Degradation of Industrial PERC, TOPCon, and HJT Solar Cells: The Next Big Reliability Challenge?," *Solar RRL* 8 (2024): 2400628.

15. H. Ye, S. Huang, C. Qian, et al., "Short Wavelength Photons Destroying Si-H Bonds and Its Influence on High-Efficiency Silicon Solar Cells and Modules," *Solar RRL* 7 (2023):

16. C. Sen, X. Wu, H. Wang, et al., "Accelerated Damp-Heat Testing at the Cell-Level of Bifacial Silicon HJT, PERC and TOPCon Solar Cells Using Sodium Chloride," *Solar Energy Materials and Solar Cells* 262, (2023): 112554.

17. P. Gebhardt, S. Marletti, J. Markert, et al., "Comparison of Commercial TOPCon PV Modules in Accelerated Aging Tests," *IEEE J. Photovoltaics* 15 (2025): 24.

18. M. Rivera and C. Reise, 41st European Photovoltaic Solar Energy Conference and Exhibition (EUPVSEC), (2024 020288–001-007, https://userarea.eupvsec.org/proceedings/.

19. R. M. Smith, D. C. Jordan, and S. R. Kurtz, World Renewable Energy Forum (National Renewable Energy Laboratory (NREL), 2012).

20. M. Theristis, J. S. Stein, C. Deline, et al., "Onymous Early-Life Performance Degradation Analysis of Recent Photovoltaic Module Technologies," *Progress in Photovoltaics: Research and Applications* 2023 (31): 149.

21. F. Maischner, W. Kwapil, J. M. Greulich, et al., "Process Influences on LeTID in Ga-Doped Silicon," *Solar Energy Materials and Solar Cells* 260 (2023): 112451.

22. P. Gebhardt, G. Mülhöfer, A. Roth, and D. Philipp, "Statistical Analysis of 12 years of Standardized Accelerated Aging in Photovoltaic-Module Certification Tests," *Progress in Photovoltaics: Research and Applications* 29 (2021): 1252.

23. D. C. Jordan, C. Deline, S. Johnston, et al., "Silicon Heterojunction System Field Performance," *IEEE J. Photovoltaics* 8 (2018): 177.

24. L. Pirot-Berson, R. Couderc, R. Bodeux, and J. Dupuis, "Failure Modes of Silicon Heterojunction Photovoltaic Modules in Damp Heat Environment: Sodium and Moisture Effects," *Solar Energy Materials and Solar Cells*. (278 (2024): 113190.

Supporting Information

Additional supporting information can be found online in the Supporting Information section.

2367198x, 2025, 16, Downloaded from https://onlinelibrary.wiley.com/doi/10.1002/solr.202500364 by Fraunhofer Ise Inst. Solar Energy Systems, Wiley Online Library on [05/11/2025]. See the Terms and Conditions (https://onlinelibrary.wiley.com/terms-and-conditions) on Wiley Online Library for rules of use; OA articles are governed by the applicable Creative Commons License